EPR Study of the Surface Characteristics of Nanostructured TiO_2 under UV Irradiation

Juan M. Coronado,*,† A. Javier Maira,† José Carlos Conesa,† King Lun Yeung,‡ Vincenzo Augugliaro,†,§ and Javier Soria†

Instituto de Catálisis y Petroleoquímica, CSIC, Campus UAM, Cantoblanco, Madrid 28047, Spain, and Department of Chemical Engineering, The Hong Kong University of Science and Technology, Clear Water Bay, Kowloon, Hong Kong

Received January 29, 2001. In Final Form: April 24, 2001

Nanostructured TiO_2 samples with primary particle size in the 4−20 nm range were prepared by either hydrothermal (H) or thermal (T) treatment of an amorphous precursor, and their behavior under UV illumination at 77 K was studied by means of EPR spectroscopy. The samples of the H series present the smallest crystallite size and after irradiation in a vacuum show some Ti^{3+} centers. In contrast, under these conditions only weak signals associated with oxygenated radicals are observed for the T samples. However, when oxygen is preadsorbed, several oxygenated complexes (O^-, O_2^-, $O_2H^\bullet$, and O_3^-) are photogenerated in proportions that depend on the characteristics of the material. Subsurface O^- species are exclusively detected in the case of the samples of the H series, whereas ozonide radicals and surface O^- are stabilized on materials with larger crystalline domains. These oxygenated complexes are thermally unstable, and they disappeared after warming to room temperature in the case of the T samples, but they are transformed to O_2^- on the surface of the hydrothermally treated TiO_2. Since adsorbed water and different types of free hydroxyls are present on these materials, as revealed by FTIR, a number of surface reactions have to be considered in order to account for the formation and stability of such photogenerated species.

Introduction

Photocatalytic oxidation (PCO) constitutes one of the most promising methods for indoor air purification. Mineralization of a number of organic pollutants can be achieved at ambient temperature and pressure, using the anatase phase of TiO_2 activated by UV irradiation.[1,2] However, reduced quantum yields, along with the generation of undesired partial oxidation products, limit the application of this technique. [2] In addition, deactivation of the photocatalysts has been observed during the PCO of certain substrates (i.e., aromatic compounds).[1,3] To overcome these limitations, different approaches have been adopted, including reactor design improvement[4] and photocatalyst modification.[5−8] In this way, incorporation of noble metals like platinum to TiO_2 leads to a remarkable increment of the PCO rate.[5,6,9,10] Improvement of charge separation by electron transfer to the metal has been early recognized as a cause of photocatalytic activity enhancement,[5,9,10] although more recently the synergetic effect of the thermal oxidation processes on platinum have been also considered.[6] On the other hand, recent reports have shown that nanostructured anatase exhibits higher activity[7,8,11,12] and selectivity[8b,12] than commercially available TiO_2 catalysts (Degussa P25). These favorable characteristics are related to the small size of the crystallites, which defines the surface area available for adsorption and decomposition of organic pollutant. The higher surface-to-bulk ratio of these ultrafine particles could favor the transfer of photogenerated charge carriers (i.e., e^- and h^+) to the adsorbed molecules.[7] However, when the size of a semiconductor decreases to an extent that the relative proportion of surface and bulk regions are comparable, the band structure became discrete, and its chemical and optical properties differ from those of the bulk material. This phenomenon is known as the quantum size effect (QSE), and its existence in nanometer-sized TiO_2 particles is controversial.[7,8,12,13] Thus, Serpone et al. proposed that this effect is not perceptible for particles larger than 2 nm,[13] whereas other authors have attributed the noticeable shifts in the electronic spectra of TiO_2 with particle size smaller than 10 nm to the QSE.[8a,12] Anyhow, the higher concentration of structural defects expected on these small crystallites could result in an increment of the electron/hole recombination rate.[11,12,14] The surface structure of these small TiO_2 particles must also play a determining role in their catalytic properties, as it has

† Instituto de Catálisis y Petroleoquímica.

‡ The Hong Kong University of Science and Technology.

§ Permanent address: Dipartimento di Ingegneria Chimica dei Processi e dei Materiali, Università degli Studi di Palermo, Viale delle Scienze, 90128 Palermo, Italy.

* Corresponding author. E-mail jmcoronado@icp.csic.es; Fax 34-91-585-47-60.

(1) Peral, J.; Ollis, D. *J. Catal.* **1992**, *136*, 554.

(2) Hoffman, M. R.; Martin, S. T.; Choi, W.; Bahnemann, D. W. *Chem. Rev.* **1995**, *95*, 69. (b) Linsebigler, A.; Lu, G.; Yates, J. T. *Chem. Rev.* **1995**, *95*, 735.

(3) Alberici, R. M.; Jardim, W. F. *Appl. Catal. B* **1995**, *14*, 55.

(4) Peill, N. J.; Hoffmann, M. R. *Environ. Sci. Technol.* **1995**, *29*, 2974.

(5) Fu, X.; Zeltner, W. A.; Anderson, M. *Appl. Catal. B* **1995**, *6*, 209.

(6) Kennedy, J. C. III.; Datye, A. K. *J. Catal.* **1998**, *179*, 375.

(7) Cao, L.; Huang, A.; Spiess, F. J.; Suib, S. L. *J. Catal.* **1999**, *188*, 48.

(8) (a) Maira, A. J.; Yeung, K. L.; Lee, C. Y.; Yue, P. L.; Chan, C. K. *J. Catal.* **2000**, *192*, 185. (b) Maira, A. J.; Yeung, K. L.; Soria, J.; Coronado, J. M.; Belver, C.; Lee, C. Y.; Augugliario, V. *Appl. Catal. B* **2001**, *29*, 327.

(9) Kraeutler, B.; Bard, A. J. *J. Am. Chem. Soc.* **1978**, *100*, 2239.

(10) Sakata, K.; Hashimoto, K.; Kawai, T. *J. Phys. Chem.* **1984**, *88*, 5214.

(11) (a) Kominami, H.; Kato, J. I.; Kohno, M.; Kera, Y.; Ohtani, B. *Chem. Lett.* **1996**, *12*, 1051. (b) Kominami, H.; Kato, J.; Takada, Y.; Doushi, Y.; Ohtani, B.; Nishimoto, S.; Inoue, M.; Inui, T.; Kera, Y. *Catal. Lett.* **1997**, *46*, 235.

(12) Zhang, Q.; Gao, L.; Guo, *Appl. Catal. B* **2000**, *26*, 207.

(13) Serpone, N.; Lawless, D.; Khairutdinov, R. *J. Phys. Chem.* **1995**, *99*, 16646.

(14) Zhang, Z.; Wang, C. C.; Zakaria, R.; Ying, Y. *J. Phys. Chem. B* **1998**, *102*, 10871.

10.1021/la010153f CCC: $20.00 © 2001 American Chemical Society
Published on Web 07/24/2001

Table 1. Synthesis Conditions and Textural Properties of the Nanostructured TiO_2 Materials Studied

sample type	sample name	crystallite size (nm)[a]	preparation conditions	BET surface area ($m^2\ g^{-1}$)	equiv particle size (nm)[b]
H	H4	3.8	15 mL of H_2O + 10 mL of 2-propanol at 100 °C for 8 h	242	5.9
	H5	5.2	15 mL of H_2O + 10 mL of 2-propanol at 150 °C for 8 h	204	6.9
	H6	6.2	12 mL of H_2O + 13 mL of 2-propanol at 150 °C for 8 h	160	8.8
T	T11	11	air at 450 °C for 3 h	93	15.2
	T16	16	air at 500 °C for 3 h	34	42
	T20	20	air at 500 °C for 12 h	13	109

[a] Size measured from XRD line broadening. [b] Calculated from BET area for a model of homodispersed spherical particles.

been found for other nanometer-sized semiconductors.[15] In this context, the characteristics of the hydroxyl groups, along with other surface processes such as the stability of photogenerated radicals and the adsorption strength of pollutants, are strongly influenced by the surface properties. Despite their importance, there is a considerable lack of information on the surface structure of nanometer-sized TiO_2, where changes in particle size is likely to results in the modification of the active sites.

In the present work, EPR spectroscopy has been used to examine the surface characteristics of a series of TiO_2 with controlled particle size varying between 4 and 20 nm, prepared by either thermal or hydrothermal treatment of an amorphous precursor. The formation of radicals upon irradiation in a vacuum or after oxygen adsorption was monitored by means of EPR, meanwhile FTIR was used to check the presence of adsorbed water and hydroxyls groups. Results obtained are discussed considering the different surface reactions in which photogenerated charge carriers, adsorbed H_2O/OH^-, and O_2 could participate. These features are discussed in connection with the structural and photocatalytic properties of the nanostructured TiO_2.

Experimental Section

Catalyst. Amorphous titania gel spheres (100 nm) were prepared by a sol−gel process described in a separate report[8] using titanium isopropoxide (Aldrich). Subsequent hydrothermal treatment (samples H) crystallizes TiO_2 in its anatase phase with sizes below 10 nm depending on the treatment conditions. To obtain larger anatase crystallites (i.e., 11−20 nm), the amorphous TiO_2 precursor was calcined at temperatures up to 773 K during different lengths of time (samples T). Table 1 summarizes the synthesis conditions for the studied catalysts along with their particle size and BET surface area. Comparison of the particle size obtained from the XRD measurements and the calculated value based on the specific surface assuming homodispersed spherical particles suggests that the thermally treated TiO_2 (i.e., samples T) exists as polycrystalline aggregates.

Catalyst Characterization. FTIR experiments were conducted in 5ZDX Nicolet spectrometer provided with a MCT detector, using a Pyrex glass cell with NaCl windows where self-supported disks (≈20 mg cm^{-2}) were placed for vacuum treatments. Spectra were recorded by accumulation of 250 scans with a resolution of 4 cm^{-1}. The EPR measurements were carried out in Bruker ER200D instrument operating in the X-band. Aliquots of the catalyst (12−30 mg) were placed into a special cell made of spectroscopically pure quartz and with greaseless taps for treatments. All the spectra were recorded at 77 K in a T-type double cavity. The frequency of the microwave was calibrated for each experiment using a standard of DPPH (g = 2.0036) located in the second cavity. Computer simulations were used when necessary to check spectral parameters and to establish the contribution of each signal to the total intensity. The adsorption and/or desorption treatments were carried out in a conventional vacuum line, achieving pressures down to 10^{-3} N m^{-2}. Irradiation treatments at 77 K were carried out placing the cell in a quartz dewar flask without any metallic coating and filled with liquid N_2. For these experiments the UV sources were three fluorescent lamps (Osram Eversun L40W/79K), which emits their maximum intensity at 350 nm.

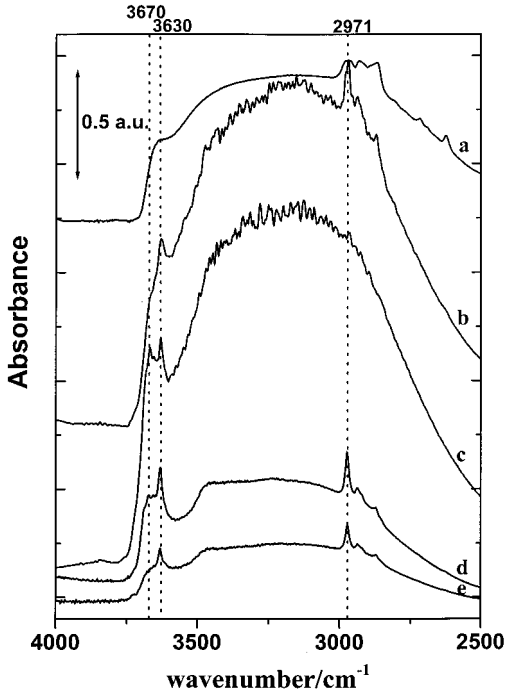

Figure 1. FTIR of self-supported disks of (a) TiO_2 gel, (b) H5, (c) H6, (d) T11, and (e) T16 samples outgassed at RT for 2 h.

Results

1. FTIR Measurements. A FTIR study of hydroxyl species was carried out on the different TiO_2 samples after vacuum degassing at room temperature for 2 h. Figure 1 shows the spectra in the 4000−2000 cm^{-1} range of some representative samples. All the studied materials, with the exception of the amorphous precursor, displayed a relatively sharp peak located at 3630 cm^{-1}, along with other bands or shoulders (depending of the specific sample) at ca. 3670 cm^{-1}, which could be assigned to the stretching mode of isolated surface OH groups with different degrees of acidity.[16] In the case of the TiO_2 gel these species give rise to a relatively broad band centered at about 3630 cm^{-1}, as expected for a less ordered environment of the OH species. A broad absorption covering the 3600−2400 cm^{-1} interval is present in all samples, but a weaker contribution at ca. 3450 cm^{-1} is also discernible in samples of larger particle size. These features can be ascribed to associated hydroxyls, from either water molecules or surface OH^- groups, that are involved in hydrogen-bonding interactions.[16] Some sharp peaks are also observed for several samples at ca. 2960, 2920, and 2850 cm^{-1}. They are ascribed to the ν(CH) modes and combina-

(15) Sakohara, S.; Ishida, M.; Anderson, M. A. *J. Phys. Chem. B* **1998**, *102*, 10169.

(16) Martra, G. *Appl. Catal. A* **2000**, *200*, 275.

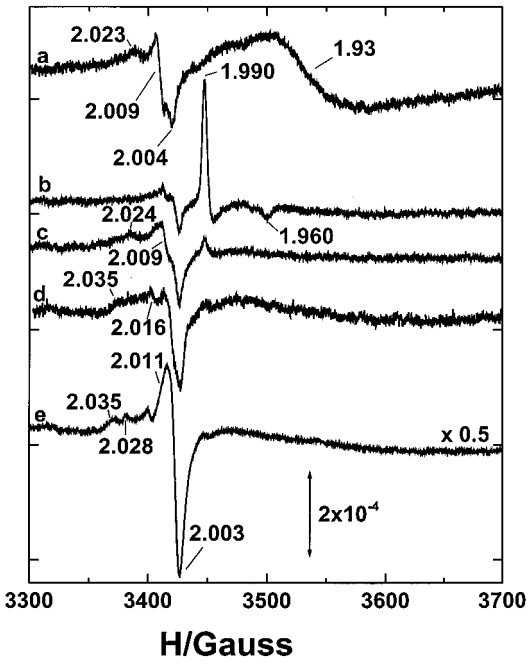

Figure 2. EPR spectra of the TiO_2 gel sample outgassed 1 h at RT and (a) irradiated for 15 min at 77 K; H6 sample treated in a vacuum for 1 h at RT and (b) subsequently irradiated during 15 min at 77 K; and (c) contacted with O_2 at 77 K; T16 material outgassed at RT for 1 h and (d) irradiated for 15 min and (e) subsequently exposed to O_2 at 77 K.

tion bands of adsorbed organic species which were not totally eliminated during the preparation procedure.

The intensity of the OH-related bands of the hydrated samples, especially for the case of the broad absorption at about 3300 cm^{-1}, is roughly related to their BET surface area. However, the decrement of the absorbance in this region with the extent of the degassing treatment (which can be related with the amount of water desorbed) seems to be relatively larger for the samples of the T series. The easier removal of adsorbed water from the surface of anatase samples treated in air at high temperature might be related to the annealing of surface defects with increasing the crystallinity of the TiO_2 samples. Concerning the sharper OH bands with frequencies above 3600 cm^{-1}, it is worth mentioning that, among the different specimens studied, the intensity of band corresponding to the more basic groups at ca. 3670 cm^{-1} was largest for the H6 sample.

2. EPR Results. *2.1. Irradiation in Static Vacuum.* The EPR spectra of the amorphous titania gel and the different sized anatase TiO_2 were recorded at 77 K after outgassing at RT for 1 h, followed by UV irradiation in static vacuum at 77 K. The spectrum obtained for the TiO_2 precursor in such way (Figure 2a) shows two features: signal R with $g_1 = 2.023$, $g_2 = 2.009$, and $g_3 = 2.004$ and a broader signal T1 with $\langle g \rangle \approx 1.93$. Signal T1 is similar to signals found in the spectra of colloidal TiO_2 after UV irradiation, which were ascribed to photogenerated Ti^{3+} centers in amorphous TiO_2.[17] The absence of this signal in all the other samples indicates that (nearly) all of the amorphous material has crystallized after the hydrothermal and thermal treatment. Signal R displays g values very close to those corresponding to $Ti^{4+}-O_2^-$ species,[18,19] although g_3 appears at slightly lower field. Considering this latter fact and how this signal was produced, it seems more likely that it corresponds to radicals formed by photoreaction of the residual organic groups, in similar way as that reported for cysteine-modified TiO_2 colloids.[21] Indeed, certain oxygenated radicals (e.g., organic peroxyls) gives similar parameters to that of signal R.[22]

After UV irradiation under vacuum at 77 K all crystallized anatase samples give rise to several weak signals, those with $g > 2.00$ are in most cases severely overlapped and difficult to deconvolute. However, some of these features appear only in either the hydrothermal or the thermally treated samples, suggesting that the formation of such species can be directly related to the way the TiO_2 was crystallized. Thus, a narrow signal T2, with $g_\perp = 1.990$ and $g_{||} = 1.960$, is observed with similar intensity in the case of the samples H, as shown in the spectrum of H6 irradiated under vacuum presented in Figure 2b. This signal has also been detected in colloidal TiO_2 anatase, and it was assigned to substitutional Ti^{3+} in hydrated anatase.[17,18,20] However, the same signal is considered a bulk species in Sb-doped anatase and can be also generated in pure titania by vacuum treatment at $T \leq 1000$ K. Therefore, it seems that water is not required to form these centers.[20] In the present case, this signal most likely corresponds to electrons stabilized in Ti cations located at crystallization defects or at surface sites where the oxygen anion is partially substituted by hydroxyls groups (i.e., $(O^{2-})_x-Ti^{3+}-(OH^-)_y$ entities). Another weak contribution that it is characterized by a maximum at $g \approx 2.010$ and a minimum at $g \approx 2.002$ is observed for samples H6 after irradiation in a vacuum (Figure 2b). This signal can be attributed to a new species, called hereafter A, which is obtained with better resolution under different conditions (see below). In the case of the calcined samples (cf. Figure 2d), the signal T2 is absent, but the modification of the spectrum baseline at the high field side suggests a broad signal that could be related to conduction electrons. At the low field side, there exists some features with relatively low intensity that have extrema at $g = 2.035$, 2.016, 2.009, and 2.003. They are assigned to at least three signals that constitute the spectra of samples T.

2.2. Adsorption of O_2 onto Preirradiated Samples. After turning off the UV lamps, oxygen was adsorbed onto the preirradiated samples and examined by EPR. The EPR spectra show again two different types of behavior that correlates well with the sample preparation method. The spectra of type H samples displayed a marked decrease in signal T2 that is accompanied by the formation of at least one new signal A, with parameters $g_1 = 2.024$, $g_2 = 2.009$, and $g_3 = 2.003$ (Figure 2c). Double integration of the different spectral features shows that the amount of spins corresponding to the new signals generated in the range $g > 2$ is similar to or slightly lower than the amount of Ti^{3+} ions that generates signal T2. In the case of the type T samples, O_2 adsorption produces a large increase in the intensity of the spectra as can be seen in Figure 2e for T16. These spectra are formed by at least three components, which are also present in the irradiated samples before oxygen adsorption but with lower intensity. These are signal B, with $g_1 = 2.035$, $g_2 = 2.009$, and $g_3 =$

(17) Howe, R. F.; Grätzel, M. *J. Phys. Chem.* **1985**, *89*, 4495.
(18) Howe, R. F.; Grätzel, M. *J. Phys. Chem.* **1987**, *91*, 3906.
(19) (a) Anpo, M.; Che, M.; Fubini, B.; Garrone, E.; Giamello, E.; Paganini, M. C. *Top. Catal.* **1999**, *8*, 189. (b) Naccache, C.; Meriaudeau, P.; Che, M.; Tench, A. J. *J. Chem. Soc., Faraday Trans.* **1971**, *67*, 506.
(20) (a) Meriaudeau, P.; Che, M.; Gravelle, P. C.; Teichner, S. J. *Bull. Soc. Chim. Fr.* **1971**, 13. (b) Meriaudeau, P.; Che, M.; Jorgersen, C. K. *Chem. Phys. Lett.* **1970**, *5*, 131. (c) Che, M.; Gravelle, P. C.; Meriaudeau, P. *C. R. Acad. Sci.* **1969**, *2868C*, 768.
(21) Rajh, T.; Ostafin, A. E.; Micic, O. I.; Tiede, D. M.; Thurnauer, M. C. *J. Phys. Chem.* **1996**, *100*, 4538.
(22) Sevilla, M. D.; Becker, D.; Yao, M. *J. Chem. Soc., Faraday Trans.* **1990**, *86*, 3279.

Table 2. Summary of EPR Parameters and Assignment of the Oxygen-Related Signals Observed, along with Literature Values Measured for Similar Species

	EPR parameters				
signal	g_1	g_2	g_3	assignment	observations
R	2.023	2.009	2.004[a]	organic peroxyl (e.g., ROO•)	formed upon γ or UV irradiation;[22,21] affected by O_2 adsorption
	2.022		2.004[21]	carboxyl radical of cysteine	
	2.035	2.008	2.003[22]	$(CH_3)_3N^+CH_2$ OO•	
A	2.024	2.009	2.003[a]	$Ti^{4+}-O_2^-$ on anatase	confirmed by ^{17}O-enriched O_2 adsorption;[19,29] formed after TiO_2 reduction or UV irradiation; requires O_2 adsorption
	2.025	2.009	2.003[18]		
	2.021	2.009	2.003[29]		
	2.024	2.009	2.003[19]		
B	2.034	2.009	2.002[a]	$Ti^{4+}-O_2H$	observed after UV irradiation of hydroxylated TiO_2;[23] EPR parameters in accordance with theoretical calculations[24]
	2.034	2.008	2.002[23]		
	2.034	2.003	2.002[24]		
C	2.028	2.016	2.002[a]	$Ti^{4+}-O^{2-}-Ti^{4+}-O^-$ (O_s^-)	formed after UV irradiation in a vacuum of partially dehydroxylated TiO_2;[27,28] affected by O_2 adsorption; it is not formed by TiO_2 reduction in a vacuum
	2.030	2.018	2.004[27]		
	2.027	2.019	2.007[28]		
D	2.011	2.007	2.002[a]	$Ti^{4+}-O_3^-$	formed after UV irradiation of partially dehydroxylated TiO_2 in the presence of O_2;[29,30] it is not formed by TiO_2 reduction in a vacuum
	2.014	2.009	2.003[29]		
	2.009	2.003	2.003[30]		
E	2.024	2.013	2.003[a]	$Ti^{4+}-O^-Ti^{4+}-OH^-$ (O_B^-)	formed after UV irradiation of hydroxylated TiO_2;[18,27,28] it is not affected by O_2; it is not formed by TiO_2 reduction in a vacuum
	2.024	2.014	2.007[28]		
	2.016	2.012	2.002[18]		
	2.018	2.014	2.004[27]		

[a] This work.

2.003, signal C, with $g_1 = 2.028$, $g_2 = 2.016$, and $g_3 = 2.002$, and signal D, with $g_1 = 2.011$, $g_2 = 2.007$, and $g_3 = 2.002$. Similar results are obtained with other samples of the T series, but some contribution of signal A can be also be envisaged. The g values of signal A and the procedure that leads to its formation (trapping of electrons from Ti^{3+} cations by O_2 molecules) indicate that it belongs to $Ti^{4+}-O_2^-$ species.[18,19] Signal B has been previously assigned to O_2H[23] radicals on the basis of theoretical calculations[24] and the comparison with results obtained in solution.[25,26] Signal C is observed when the large TiO_2 particles are UV-irradiated under vacuum, and it vanishes in the presence of an excess of adsorbed O_2. These radicals have been assigned to surface O^- species;[27,28] and it will be referred in this paper as O_S^-. Finally, signal D observed for UV-irradiated type T samples in the presence of oxygen has been assigned to O_3^- radicals.[29,30] The parameters of the different signals assigned to oxygenated species, along with the literature values, are collected in Table 2.

2.3. Irradiation in the Presence of Adsorbed O_2. After exposing the preirradiated samples to oxygen at 77 K and obtaining their EPR spectra in the dark, the samples were irradiated with UV at 77 K in the presence of the adsorbed O_2 and the EPR spectra were collected and displayed in Figure 3. Computer simulations (dotted lines) show that the spectra of samples H can be fairly well reproduced considering three overlapped signals (A, B, and E), while four overlapped signals (A, B, C, and D) were required for samples T. Signals similar to E have been reported for

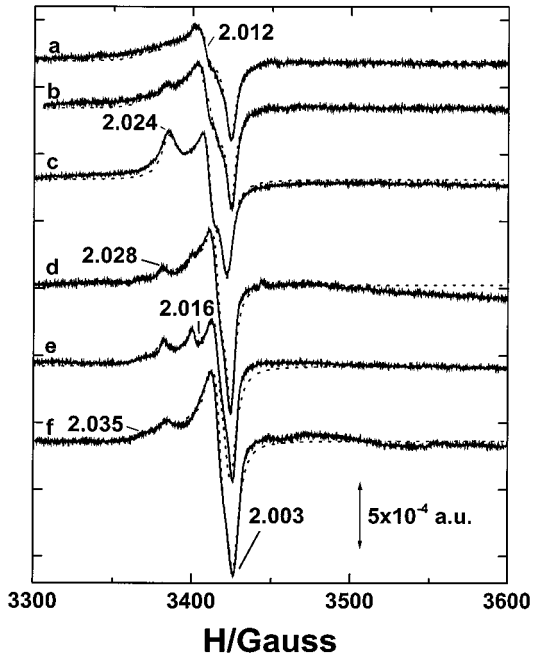

Figure 3. EPR spectra of the (a) H4, (b) H5, (d) T11, (e) T16, and (f) T20 materials treated in a vacuum at RT for 1 h, contacted with O_2 at 77 K, outgassed for 15 min, and irradiated for 15 min at the same temperature; (c) the P5 material subsequently heated at RT.

UV-irradiated colloidal TiO_2 and anatase samples with small particle size.[18,27,28] In addition, some of the poorly resolved features at $g > 2$ observed when H samples are illuminated in a vacuum correspond very likely to the E species. Since separate experiments show that this signal does not broaden during the adsorption of oxygen in excess, it must correspond to nonsuperficial species. Accordingly, it has been assigned to photogenerated holes trapped by subsurface lattice oxygens, giving O^- species which might be stabilized by surface OH^- groups.[27,28] Such species will be denoted here as O_B^-, and they can be fairly well reproduced using the following parameters: $g_1 = 2.024$, $g_2 = 2.013$, and $g_3 = 2.003$. Although computer simulation yields a higher g_1 value than those reported in the literature, extrema of signal E (maximum at $g = 2.018$

(23) López Muñoz, M. J.; Soria, J.; Conesa J. C.; Augugliaro, V. *Stud. Surf. Sci. Catal.* **1994**, *82*, 693.
(24) McCain, D. C.; Palke, W. E. *J. Magn. Reson.* **1975**, *20*, 52.
(25) Wyard, S. J.; Smith, R. G.; Adrian, F. J. *J. Chem. Phys.* **1968**, *49*, 2780.
(26) Riederer, H.; Hüttermann, J.; Boon, P.; Symons, C. R. *J. Magn. Reson.* **1983**, *54*, 54.
(27) Nakaoka, Y.; Nosaka, Y. *J. Photochem. Photobiol. A* **1997**, *110*, 299.
(28) (a) Micic, O. I.; Zhang, Y.; Cromack, K. R.; Trifunac, A. D.; Thurnauer, M. C. *J. Phys. Chem.* **1993**, *97*, 7277. (b) Micic, O. I.; Zhang, Y.; Cromack, K. R.; Trifunac, A. D.; Thurnauer, M. C. *J. Phys. Chem.* **1993**, *97*, 13284.
(29) Meriaudeau, P.; Vedrine, J. C. *J. Chem. Soc., Faraday Trans.* **1976**, *72*, 476.
(30) Anpo, M.; Kubokawa, Y.; Fujii, T.; Suzuki, S. *J. Phys. Chem.* **1984**, *88*, 2572.

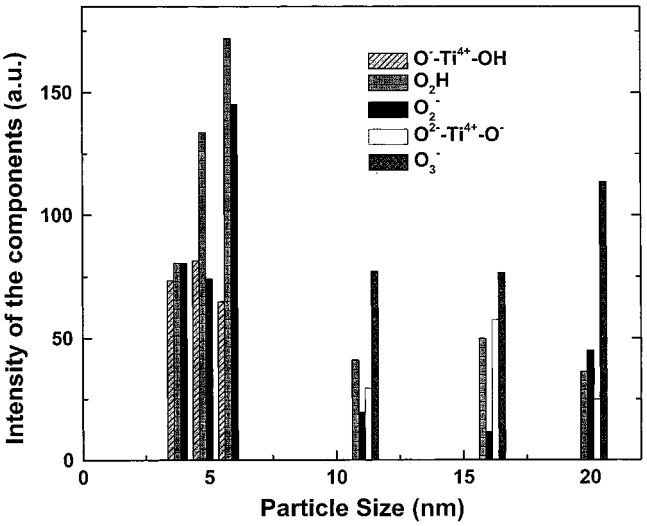

Figure 4. Bar diagram of the contribution of each signal to the EPR spectra shown in the former figure, obtained from the computer simulations and corrected by the number of spins.

and minimum at $g = 2.004$) are basically coincident with previous results. Nevertheless, the value of the g_1 component cannot be determined with total accuracy due to its considerable broadening. The proportion of each signal used for the computer simulation of the spectra, corrected by the number of spins obtained by double integration, is shown in the bar diagram of Figure 4. These data show that the maximum density of photoproduced oxygenated radicals correspond to the samples with particle size of 6 nm. There is a remarkable difference in the TiO_2 prepared by thermal and hydrothermal treatments. All the radicals observed in the T-type samples disappears after the sample was heated to room temperature, but for the H-type samples superoxide species are formed after warming (Figure 3). Since double integration of the signals reveals that the number of spins remains almost constant during this process, it is likely that all the species detected at 77 K are transformed at room temperature to O_2^- complexes on the surface of the H-type materials. Another distinction between the two types of samples is observed when the spectra described in this section (Figure 3) are compared with those obtained after O_2 adsorption in the dark on samples previously irradiated under vacuum (e.g., Figure 2c,e). In the case of T samples the signals contributing to the spectra obtained in both types of experiment are basically the same, and the intensity increases moderately upon oxygen admission. In contrast, for samples H the spectral amplitude is markedly larger when irradiation is carried out in the presence of adsorbed oxygen than when UV illumination is carried out before gas adsorption.

Discussion

The interpretation of the EPR data observed in this study can be made using the well-established reaction scheme know to occur during the UV irradiation of anatase TiO_2. The absorption of photons leads to the generation of electron−hole pairs (either associated in excitons or as free carriers) in the bulk oxide:[17−19,27,28]

$$TiO_2 + h\nu \rightarrow TiO_2\,(h^+ + e^-) \quad (1)$$

These charge carriers can be trapped at several centers: the electrons in Ti^{4+} ions (at the bulk or the surface)[17,18]

$$Ti^{4+} + e^- \rightarrow Ti^{3+} \quad (2)$$

and holes at bulk or surface anions (neutral radicals are marked by "•"):[18,27,28]

$$Ti^{4+}-O^{2-}-Ti^{4+}-OH^- + h^+ \rightarrow Ti^{4+}-O^--Ti^{4+}-OH^-\ (O_B^-\ \text{species}) \quad (3)$$

$$Ti^{4+}-OH^- + h^+ \rightarrow Ti^{4+}-OH^\bullet \quad (4)$$

$$Ti^{4+}-O^{2-} + h^+ \rightarrow Ti^{4+}-O^- \quad (5)$$

When O_2 molecules are present, as is the case of part of the experiments presented here, they also participate in the charge carrier trapping processes, generating surface ozonide ions[29,30]

$$Ti^{4+}-O^- + O_2 \rightarrow Ti^{4+}-O_3^- \quad (6)$$

and superoxide species[18,19]

$$Ti^{3+} + O_2 \rightarrow Ti^{4+}-O_2^- \quad (7)$$

These latter radicals can capture protons, when available:

$$Ti^{4+}-O_2^- + H^+ \rightarrow Ti^{4+}-O_2H^\bullet \quad (8)$$

The extent of this process, which is actually an equilibrium, will depend on the Brönsted acidity of the surface.

Consequently, among EPR-detectable species Ti^{3+}, O_2^-, and $O_2H^\bullet$ may be considered in principle to reflect the production of photogenerated electrons and O^-, $OH^\bullet$, and O_3^- that of holes. The total amount of the species of the first kind consequently should balance that of the second one. The actual situation is however more complex. First, it is possible that some electrons may remain delocalized and thus produce very broad, undetectable signals. Second, some of the considered radicals may undergo secondary reactions to produce diamagnetic species or other radicals through reactions such as[31]

$$2OH^\bullet \rightarrow H_2O_2 \quad (9)$$

$$H_2O_2 + OH^\bullet \rightarrow O_2H^\bullet + H_2O \quad (10)$$

$$O_2H^\bullet + OH^\bullet \rightarrow H_2O + O_2 \quad (11)$$

$$2OH^\bullet + O_2 \rightarrow 2O_2H^\bullet \quad (12)$$

Since $OH^\bullet$ radicals are very reactive (indeed they are not normally observed in these experiments[28]), reactions such (9) to (12) will occur easily, especially when the recombination processes are in some way hindered. In addition, it must be taken into account that any organic impurity at the surface is a potential reactant for the photogenerated charge carriers, specially for holes or hole-derived species, due to the strongly oxidizing character of these latter. Besides $O_2H^\bullet$ species may also appear from photogenerated holes (by reactions 4, 9, 11, and 12), not only from electrons (by reactions 7 and 8). On the other hand, continued capture of photogenerated electrons can also originate diamagnetic species

$$O_2^- + e^- \rightarrow O_2^{2-} \quad (13)$$

(31) González Elipe, A. R.; Munuera, G.; Soria, J. *J. Chem. Soc., Faraday Trans.* **1979**, *75*, 748.

and depending on the Brönsted acidity of the surface can lead to the generation of hydrogen peroxide species:

$$O_2^{2-} + 2H^+ \rightarrow H_2O_2 \quad (14)$$

The formation of these adsorbed peroxides on the surface of the samples of the H series could account for the thermal transformation of the photogenerated O_B^- radicals into superoxide species, according to the following scheme:

$$O_2^{2-} + O^- \rightarrow O^{2-} + O_2^- \quad (15)$$

This process can be also envisaged as the transfer of a hole to the surface peroxides.

Finally, in the interpretation of these results it has to be also considered that O_2 molecules may be formed by photodesorption processes; basically, by evolution from hole-related species[18] according to reaction such as (11) or

$$O_2H^\bullet \rightarrow H_2O_2 + O_2 \quad (16)$$

$$2H_2O_2 \xrightarrow{h\nu} 2H_2O + O_2 \quad (17)$$

The adsorption of the so-produced O_2 can give O_3^-, O_2^-, or $O_2H^\bullet$. These species can appear even in the absence of O_2. In addition, the location of the photogenerated electrons at surface Ti ions, even if they remain bound a limited time, could weaken the bond between these ions and undissociated water molecules which may be adsorbed on them, leading to photodesorption of water, as has been proposed to occur.[31,32] Within the framework of all these possible processes, an analysis of the experimental results could give invaluable insight on the various factors that influence the evolution and reactivity of these photoproduced species.

Formation of Ti^{3+}. A first observation relates to the Ti^{3+} ions formed upon irradiation in a vacuum: in the amorphous precursor, they appear in the spectrum with a very broad shape, suggesting a highly heterogeneous environment or/and a fast spin relaxation rate (which could arise, for example, from a relatively symmetric octahedral coordination or a tetrahedral geometry). This fact contrasts with the much sharper T2 signal found on crystallized anatase samples of H type, which indicates a much more regular environment of axially distorted octahedral nature. This T2 signal has lower integrated intensity than signal T1, and it does not appear in samples T. However, an inverse correlation between anatase crystallinity and the amplitude of T2 signal cannot be established as similar features are detected for other well-ordered TiO_2. It is important to note that although for certain TiO_2 samples the T2-type signals have been ascribed to bulk species in anatase TiO_2,[20] in this study they correspond to Ti^{3+} ions located at the surface or within few monolayers of the surface as indicated by their rapid extinction upon introduction of oxygen. These considerations support the assignment of the T2 species to centers of the type $(O^{2-})_x-Ti^{3+}-(OH^-)_y$. Besides having small crystal sizes, samples H were not subjected to high annealing temperatures. Therefore, it is expected that in these samples will present a greater proportion of exposed Ti^{4+} cations located at crystal edges, steps and corners, that could play an important role on these catalysts' behavior. Those particular Ti^{4+} cations have a significantly lower number of lattice oxygen ions in their coordination sphere (which in hydrated samples will be partly substituted by OH^- groups and/or water), presenting appropriate characteristics for trapping electrons. For samples T that are more crystalline, a certain delocalization of the photogenerated charge carriers into extended band states, dominated by the contribution of titanium d orbitals, can take place. Strong interaction of such electrons would prevent the observation of Ti^{3+} signals as a consequence of the line broadening. In this way, it is tempting to relate the broad baseline modification observed in Figure 2d to conduction electron states. Nevertheless, this feature is scarcely affected by oxygen adsorption, and therefore it is unlikely that it can be ascribed to electrons. One should note here that, in the samples H containing the smaller crystallites, the characteristics of the delocalized electron states may be affected by quantum confinement effects, as indicated by the shift in their electronic spectra.[8a]

Trapping of Electrons in Oxygenated Radicals. A second stage of electron trapping occurs when O_2 is adsorbed on the irradiated material. In the case of samples H, most of the electrons captured by the titanium cations are transferred to the oxygen molecules to produce O_2^- and possibly a smaller amount of $O_2H^\bullet$ radicals. It is remarkable that the spectra of samples T do not show any signal attributable to isolated Ti^{3+}, but still a significant amount of $O_2H^\bullet$ is produced after exposing these preirradiated samples to oxygen. This suggests that illuminated samples may contain, after the UV emission has ceased, "active" electrons in states which are not detectable by EPR as Ti^{3+} centers but can be transferred in the dark to O_2 molecules. However, the reaction of molecular oxygen with peroxides formed according to (13) could also account for this observation. Another aspect that is worth mentioning is that, although the signals with $g > 2$ obtained after UV activation in a vacuum are very weak, some of them could still be assigned to O_2^- and/or O_2H (e.g., Figure 2d) even if adsorbed oxygen is absent. This result implies that some of these species are indirectly produced according to the reactions 4, 9, 10, 11, and 12.

On the other hand, the presence of oxygen during irradiation, when both electrons and holes are being continuously photogenerated, would promote the formation of $O_2^-/O_2H^\bullet$ species. The ratio between both types of electron-rich radicals would depend on the Brönsted acidity of the surface, although no clear tendency can be envisaged. Superoxide species are specially stable on the surface of the hydrothermally obtained materials (Figure 3c). As mentioned above, this fact may be connected with the previous formation of diamagnetic O_2^{2-} species, which upon warming to room temperature would react with the O_B^- to yield superoxide complexes. Assuming that only primary processes take place, electron-related radicals appear in larger amounts in samples H. Considering that the samples of the H series with larger crystalline size show the maximum photoactivity,[8] a correlation between the PCO rate and the increment in the surface density of such radicals could be presumed. Although the increment of the surface-to-bulk ratio favors the stabilization of photogenerated radicals, the low crystallinity of the TiO_2 samples with small particle size could increase the $e-h^+$ recombination. These opposite tendencies should result in a critical size for which the photocatalytic activity reaches a maximum. In the case of H samples, previous studies have shown that this maximum PCO rate is achieved for TiO_2 particles with 6−7 nm diameter.[8a]

Trapping of Holes. The present data show that irradiated H-type samples form subsurface O_B^- species that do not react with oxygen at 77 K, while the T-type

(32) Munuera, G.; Rives-Arnau, V.; Saucedo, A. *J. Chem. Soc., Faraday Trans.* **1979**, *75*, 136.

samples produce surface O_S^- radicals, which signals are broadened by O_2 adsorption. This implies a different location of the trapped holes for each series of samples that can be compared with the difference between both types of materials regarding Ti^{3+} generation. This fact suggests that the stabilization of photoproduced electrons and O_B^- species can be associated with similar surface structures (i.e., titanium centers with reduced oxygen coordination). A remarkable feature of the H samples is that after UV irradiation in absence of oxygen only weak O_B^- signals are detected. This behavior contrasts with previous reports of the literature that show that O^- species can be readily generated upon illumination in a vacuum.[27,28] Capture of holes by residual organic groups to lead to diamagnetic species (or small amounts of R species) could partly account for this experimental observation. However, the stabilization of the O_B^- radicals after oxygen admission suggests the existence of additional mechanisms. A fraction of the photoproduced holes reaching the surface of these highly hydroxylated samples should react with surface OH^- groups to generate very reactive $OH^\bullet$ radicals (reaction 4). If adsorbed molecules are absent these radicals are expected to form diamagnetic H_2O_2 molecules (i.e., reaction 9) that subsequently react to form $O_2H^\bullet$, H_2O, or O_2 (i.e., reactions 10 and 15). On the contrary, if adsorbed oxygen is present, it can further react with the adsorbed peroxide according to

$$O_2^{2-} + O_2 \rightarrow 2O^- + 2O^{2-} \qquad (18)$$

It is worth noting that O_2^{2-} can be also formed from the capture of electrons (i.e., reaction 13). Anyhow, process 18 could explain the formation of O_B^- and O_S^- radicals after oxygen exposure and subsequent UV irradiation. However, ozonide species are not formed on the surface of samples H, although a mechanism similar to (19) (see below) could account for the generation of O_3^- on thermally treated materials. This fact suggest that the surface of samples H lacks of the sites (possibly some kind of basic O^{2-}) required to stabilize these radicals.

Although the signals obtained from the samples after UV irradiation in a vacuum are poorly resolved, a clear comparison can be made on the two kinds of samples after the adsorption of oxygen in the dark. It was observed that the amplitude of the signals corresponding to the species generated from holes is significantly higher after oxygen adsorption for samples T. However, there is not apparent intensity change for samples H. These results suggest that, as in the case of photogenerated electrons, after irradiation has ceased most of the positive charge carriers are recombined for samples H, while in samples T a significant number of these charge carriers remain "active" in some EPR-undetectable state. The nature of this EPR-silent but O_2 reactive hole state is unclear. Delocalized holes in the valence band could account for the generation of such species, but its stabilization is extremely unlikely since their trapping in surface oxygen ions (leading to O_S^- radicals) seems rather easy. An alternative explanation is to consider a possible reactive O_2^{2-} species (or their protonated form) that could split upon interaction with O_2 in a process akin to

$$O_2^{2-} + O_2 \rightarrow O^- + O_3^- \qquad (19)$$

As mentioned above, peroxides are most likely also formed on the surface of H samples, but in the absence of oxygen they must quickly yield undetectable diamagnetic species and consequently no O_B^- species are formed in the dark.

Concluding Remarks

Significant differences between nanocrystalline TiO_2 specimens prepared hydrothermally at temperatures below 450 K (samples H) and via calcination in air at 723 K or above (samples T) from the same amorphous precursor are observed with respect to UV irradiation-induced generation of paramagnetic centers. Hydrothermal samples, which may be prepared with specific surface areas above 200 $m^2\ g^{-1}$, contain sites probably associated with defects or surface irregularities which are able to trap the photogenerated charge carriers (electron and holes), while calcined samples seem more able to keep charge carriers in EPR-silent states which, however, can produce oxygenated radicals upon subsequent O_2 adsorption. If irradiation is carried out in the presence of a electron scavenger like O_2, this molecule competes effectively with recombination, so that a higher amount of radicals is formed in the presence of this molecule. Subsurface O^- are exclusively found in samples H; meanwhile, ozonide radicals are only detected for more crystalline T samples. In the case of hydrothermal specimens their distinct properties are not simply derived from their higher surface area, but also result presumably from the higher curvature/roughness of the surface, which apparently also results in a higher stability of the surface OH^- groups and the adsorbed water. These surface characteristic may be important in determining the recently reported[8] variations in photocatalytic activity of the different titania samples.

Acknowledgment. This investigation has received financial support from ECSC (Project 7220-EB/004) J.M.C. thanks the Comunidad Autónoma de Madrid for the award of a postdoctoral grant. We also acknowledge Mr. F. Sánchez Constenla by performing some of the EPR measurements.

LA010153F